Journal of Engineering Physics and Thermophysics, Vol. 75, No. 6, 2002

NUMERICAL SIMULATION OF NONSTATIONARY TURBULENT FLOW AROUND AN AUTOMOBILE PROFILE NEAR A MOBILE SCREEN

S. A. Isaev,[a] **N. A. Kudryavtsev,**[a]
A. E. Usachev,[b] **and V. B. Kharchenko**[a]

UDC 532.517.4

A numerical investigation of nonstationary turbulent flow of an incompressible viscous fluid around the profile of a Volkswagen automobile near a mobile screen has been carried out on the basis of solution of the Reynolds equations closed using a two-parameter dissipation model of turbulence by the finite-volume method.

1. In the last few years, numerical investigations of flow around an automobile profile near a mobile screen [1–4] have been of constant interest. On the one hand, this problem is a testing area for methodological experiments on testing computational algorithms, and on the other, analysis of the vortex dynamics in the wake of a body in the neighborhood of the screen is necessary for improving the aerodynamic characteristics of automobiles. The influence of viscosity on the stationary flow of an incompressible fluid around a two-dimensional profile near a mobile screen in the laminar and turbulent regimes has been investigated in [3].

Numerical simulation of the cyclic process of formation and evolution of the von Kármán vortex street in the turbulent wake of a two-dimensional automobile profile is a central problem in the present work. We continue, to a certain extent, the investigations of [1–3] and generalize them to the case of nonstationary flow around a profile. At the same time, of particular interest is to study the regularities of vortex formation near a body of complex geometry in the presence of a mobile screen. As is known [4–7], a fairly large amount of experience in solving numerically the problems of nonstationary turbulent flow around bodies has been gained with the use of a circular cylinder; therefore, it makes sense to use it in the present work.

2. The methodology of numerical simulation of two-dimensional nonstationary flow of an incompressible viscous fluid around a body of arbitrary geometry is based on solution, within the framework of splitting by physical processes, of an initial system of Reynolds equations which is closed using a two-parameter dissipation model of turbulence [8]. Analysis of turbulent flow with developed circulation zones at high Reynolds numbers is carried out within the framework of a modified phenomenological approach that involves the introduction of eddy viscosity and allows for the influence of the curvature of streamlines on the characteristics of turbulence in accordance with the Leschziner–Rodi concept. The high-Reynolds version of the modified model is used in combination with the Launder–Spalding method of near-wall functions.

A system of master equations in divergent form is written in curvilinear coordinates matched with the contour of the body in flow for increments of dependent variables: Cartesian components of velocity, pressure, and characteristics of turbulence (kinetic energy of turbulent pulsations and rate of dissipation of turbulent energy). Discretization of the differential equations is carried out by the finite-volume method on an H-type curvilinear orthogonal grid generated based on an original elliptical procedure [2]. In this case, discrete analogs of the nonstationary terms are incorporated on the explicit side of the difference equations.

A computational algorithm for solving the problem is implemented in global time iterations involving the SIMPLEC procedure of pressure correction at each time step, which in turn is subdivided into a number of computational blocks. At the predictor stage, preliminary components of the velocity for "frozen" pressure fields and characteristics of turbulence are determined, and at the "corrector" stage, pressure is corrected on the basis of the solution of

[a]Academy of Civil Aviation, St. Petersburg, Russia; email: isaev@SI3612.spb.edu; [b]State Unitary Enterprise "State Scientific-Research Center of Central Aerohydrodynamics Institute (TsAGI)," Moscow, Russia. Translated from Inzhenerno-Fizicheskii Zhurnal, Vol. 75, No. 6, pp. 94–99, November–December, 2002. Original article submitted April 17, 2002.

1062-0125/02/7506-1363$27.00

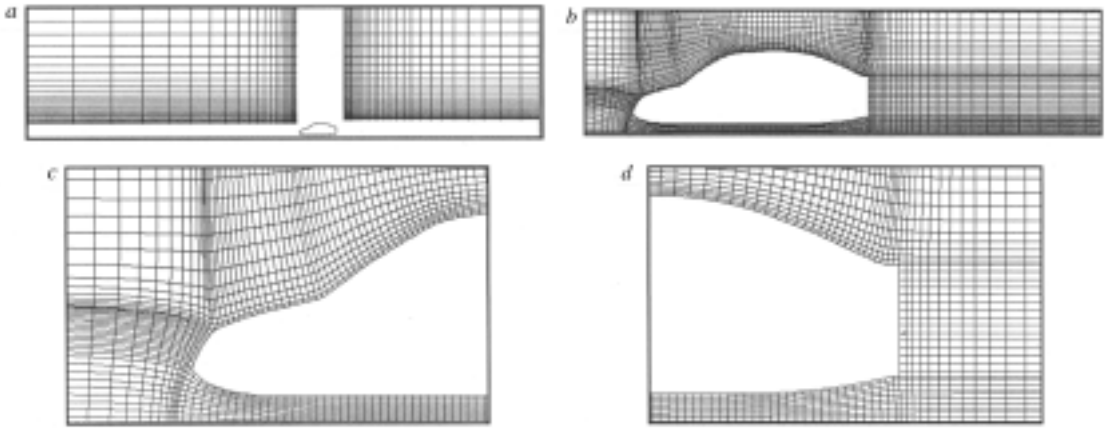

Fig. 1. Fragments of the H-type orthogonal computational grid around the profile of complex geometry near the mobile screen (the entire computational region (a) and its central part (b) and the leading (c) and trailing (d) neighborhoods of the profile).

the continuity equation with subsequent corrections of the velocity field and calculation of the characteristics of turbulence and eddy viscosity.

The selection of the centered template with fixation of dependent variables to the center of the computational cell allows one to substantially simplify the algorithm for calculating flows on curvilinear grids and reduce the number of computational operations. The monotonization or regularization of the pressure field, which is necessary in this approach, is carried within the framework of the Rhie–Chow approach [1, 5].

A high stability of the computational procedure is ensured by using one-sided upwind differences for discretization of the convective terms of the equations on the implicit side and by damping nonphysical oscillations through the introduction of artificial diffusion. The calculation efficiency of the computational algorithm increases when the method of incomplete matrix factorization is used for solving systems of nonlinear algebraic equations. Rather high accuracy of the computational procedure is determined by discretization of the explicit side of the equations by the scheme of second order of approximation, including discretization of the convective terms of the equations by Leonard's quadratic upwind scheme. Such an approach allows minimization of the effects of "numerical" diffusion that are especially substantial in calculating separated flows.

At each time step, the system of the initial discrete equations written in increments of dependent variables is solved to the attainment of an acceptable degree of convergence of the local iteration process (associated with the fulfillment of the following condition: the maximum changes in the velocity and the pressure must not exceed the selected low value of the order of 10^{-4}). Discretization of the time derivatives is carried out using the Euler difference scheme.

3. For solving the problem of two-dimensional flow around an automobile profile, the H-type multiblock grid close to an orthogonal monoblock grid (Fig. 1) (with a rectangular cut at the center of the curvilinear computational region) has been selected. The computational region is divided into 150×60 nonniformly distributed cells. The automobile contour accounts for 15 cells in the transverse direction and 81 cells in the longitudinal direction. The inlet boundary is set at a distance of 7.5 chords of the automobile profile taken as the characteristic dimension in this problem. The outlet boundary lies at a distance of 5.6 from the profile. The vertical dimension of the computational region is 3.39, the clearance is 0.06, and the thickness of the automobile profile is 0.3.

A uniform flow, which simulates the flow in the working part of a subsonic wind tunnel, is set at the inlet boundary. At the upper and outlet boundaries, "mild" boundary conditions are specified. The conditions which correspond to the mobile screen are set at the lower boundary, i.e., a solid wall moves with the velocity of an incoming flow, which is taken as the characteristic velocity. The conditions of start of the automobile profile considered with a constant velocity are taken as the initial ones. It should be emphasized that the boundary conditions set are identical to the conditions formulated in [1–3], under which the stationary problem of flow around a profile has been solved. As the dimensionless scales, in addition to the velocity of the incoming flow, we have selected the density and vis-

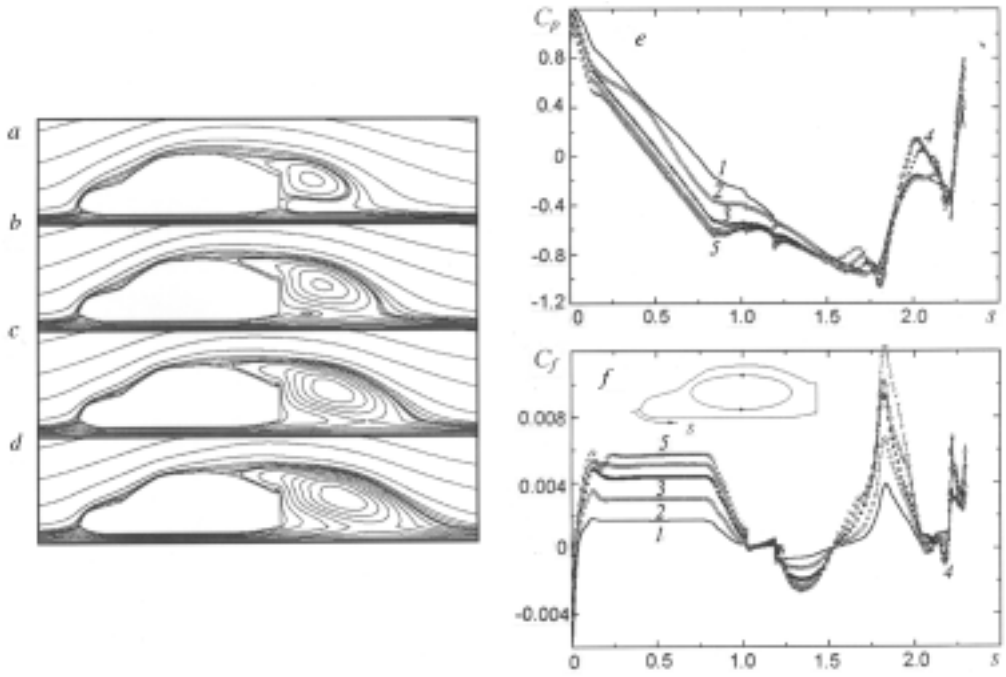

Fig. 2. Evolution of the vortex structures in the wake of the automobile profile (a–d) and the distributions of the pressure coefficient C_p (e) and the coefficient of friction C_f (f) over the contour of the profile in the first initial phase: a) t = 0.05, b) 0.15, c) 0.3, and d) 0.45 [1) t = 0.05, 2) 0.1, 3) 0.2, 4) 0.3, and 5) 0.4].

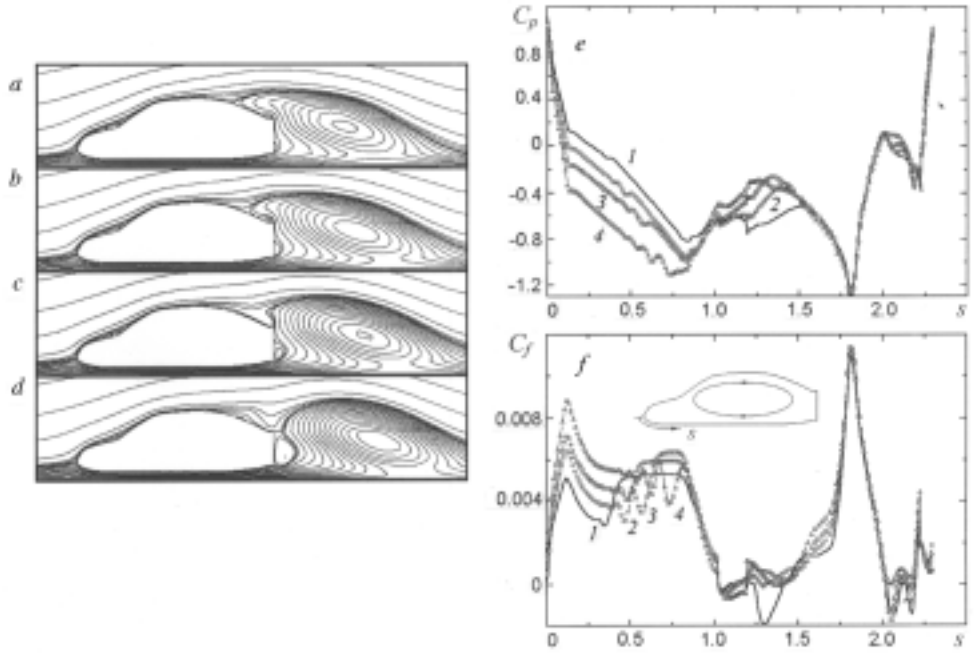

Fig. 3. Evolution of the vortex structures in the wake of the automobile profile (a–d) and the distributions of the pressure coefficient C_p (e) and the coefficient of friction C_f (f) over the contour of the profile in the second initial phase: a) t = 0.6, b) 0.75, c) 0.9, and d) 1.15 [1) t = 0.6, 2) 0.75, 3) 0.9, and 4) 1.15].

cosity of the medium and the chord of the profile. We note that the dimensionless time is determined in fractions of the ratio between the chord and the velocity of the incoming flow.

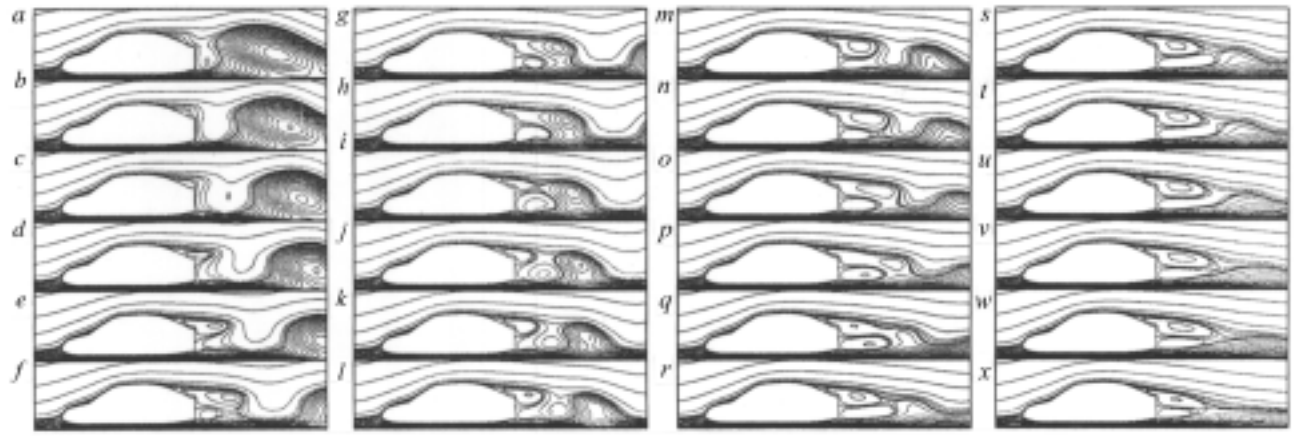

Fig. 4. Evolution of the vortex structures in the wake of the automobile profile in the transient process: a) t = 1.2; b) 1.35; c) 1.5; d) 1.65; e) 1.8; f) 1.95; g) 2.05; h) 2.15; i) 2.25; j) 2.35; k) 2.45; l) 2.55; m) 2.65; n) 2.97; o) 3.17; p) 3.37; q) 3.57; r) 3.77; s) 3.97; t) 4.17; u) 4.67; v) 5.47; w) 6.17; x) ∞ (stationary flow [3]).

Figures 2–6 sum up some results of calculation of turbulent nonstationary flow around a profile of complex geometry, representing a two-dimensional model of a Volkswagen automobile, in the vicinity of a mobile screen at Re = 10^6. The development of the process of flow is analyzed by: (a) instantaneous patterns of streamlines determined from the calculated instantaneous fields of the longitudinal velocity component, (b) graphs of contour distributions of the surface pressure coefficient and the coefficient of friction, and (c) time dependences of the intensities of vortices and integral force loads on the profile.

The initial phase of development of the process of vortex formation in the case of flow around the automobile profile, covering the period of time from 0 to 0.4 (Fig. 2 and Fig. 6a), is characterized, first of all, by the formation of the so-called starting large-scale vortex. Noteworthy is the fact that the position of the separation point on the upper surface of the profile changes only slightly at this stage, while the length of the separation zone and the intensity of flow in it increase markedly, which, in particular, follows from the progressing increase (in absolute value) in the friction stress on the rear side (bevel) of the profile. As the starting vortex develops, the level of rarefaction in the bottom region increases, while in the forepart of the body (before the windshield of the automobile), on the contrary, the pressure increases due to the retardation of the flow.

Judging from the distributions of C_f, in the clearance between the profile and the screen there arises flow with increase in the shear stress with time, as in the case of the steady-state regime of flow [3]. A characteristic feature of $C_f(s)$ is the existence of the C_f "shelf" in the clearance of constant cross section. At the exit from the gap, where the flow section is increased, the flow is naturally retarded and the friction decreases. Except for the very beginning of the process (t = 0.1), the pressure in the channel decreases linearly as the bottom region is approached. Although the pressure drop between the inlet and outlet cross sections of the clearance remains nearly constant, the flow rate and, consequently, the velocity in the gap increase by a linear law (curve 1 in Fig. 6a). It must also be noted that the acceleration of the flow on the convex part of the profile increases with time.

The second phase of development of the process (Fig. 3) is characterized by the beginning of the drift of the starting vortex to the region of the near wake and covers the period of time from 0.4 to 1.05; at the end of the zone, the trailing vortex separates practically completely from the sharp-pointed trailing edge of the profile. During the indicated period, the separation point moves gradually along the oblique wall of the profile; in this case, the intensity of the starting vortex continues to increase linearly (curve 2 in Fig. 6a). The flow rate in the clearance between the profile and the mobile screen also increases linearly (curve 1).

It is of greatest interest to track the changes in the distributions of the pressure coefficient and the coefficient of friction over the contour, because they show features that were not observed earlier in static problems. First of all, noteworthy is the distribution of the pressure disturbances and the shear stresses in the clearance. The initiation of them may be related to the moment of very sharp transformation of the separation zone on the profile, i.e., to the

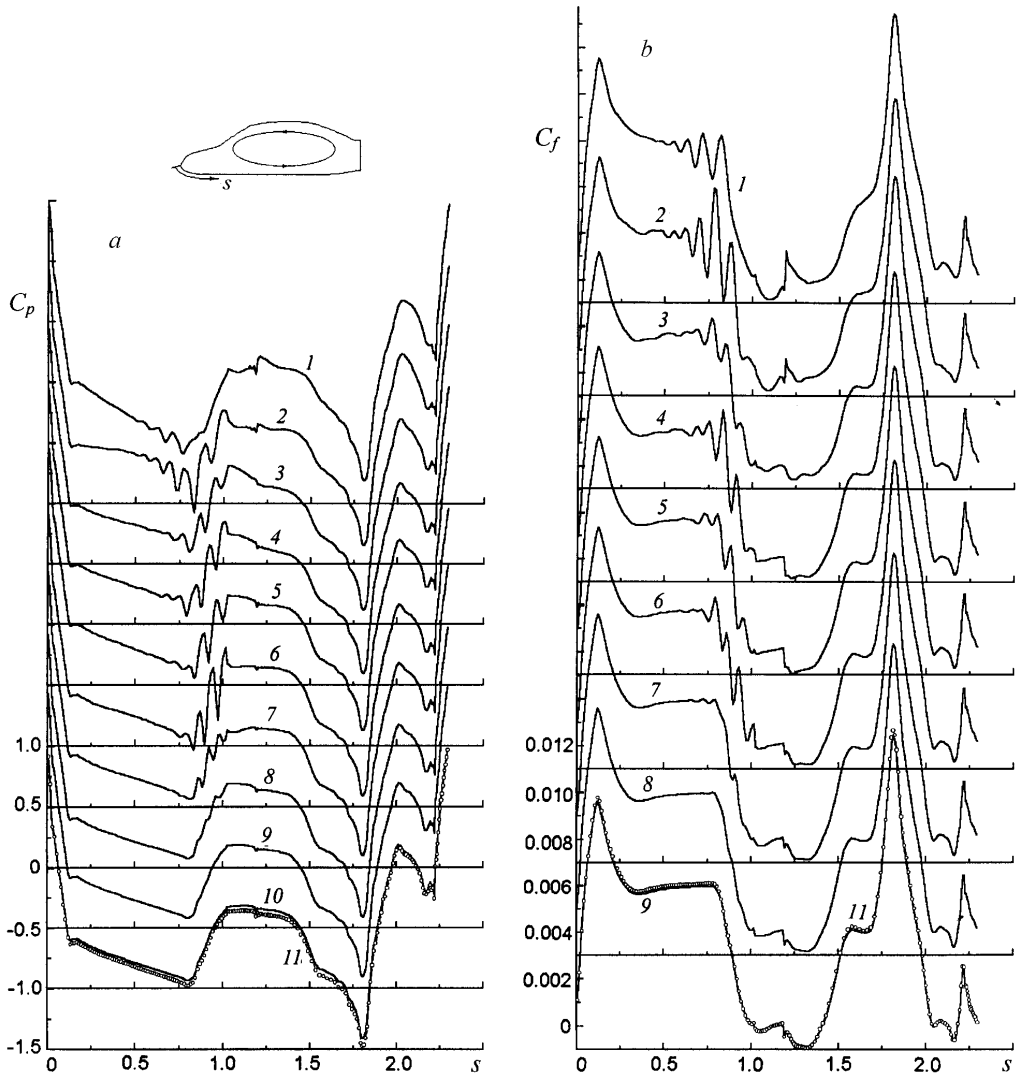

Fig. 5. Comparative analysis of the distributions of the pressure coefficient (a) and the coefficient of friction (b) over the contour of the profile at the instants of time 1) t = 1.2, 2) 1.35, 3) 1.5, 4) 1.65, 5) 1.8, 6) 1.95, 7) 2.15, 8) 2.35, 9) 2.5, 10) 2.75, and 11) 6.17.

rapid beginning of motion of the separation point. This can be judged from the fact that the dependences $C_f(s)$ change stepwise on passage from t = 0.4 to t = 0.6. As is seen, the friction increases rapidly at the entrance to the clearance, which is a consequence of the change in the pattern of flow around the nose part of the profile. As a result, there arises a very weak disturbance that begins to propagate downstream along the lower part of the contour with a gradually increasing amplitude. If the pressure wave generated in such a way begins to be seen only by the end of the period considered, the friction wave is sharply defined even at the beginning of it, and by the instant t = 1.05 the disturbance wave reaches the end of the gap channel of constant cross section.

It should be noted that the shape of $C_f(s)$ on the convex part of the profile remains nearly constant during the entire period considered, while in the region of the leading critical point the maximum of C_f increases monotonically. Yet another curious peculiarity is related to the flow around a concavity (before the windshield) in the forepart of the profile, where the retardation of the flow is accompanied by the appearance of a thin separation zone.

A further process of vortex formation and redistribution of local force loads on the airfoil is represented in Figs. 4 and 5. It makes sense to analyze the initiation, development, and disappearance of large-scale vortices in combination with the graph of the vortex intensity as a function of the time (Fig. 6a). It is seen that the largest starting vor-

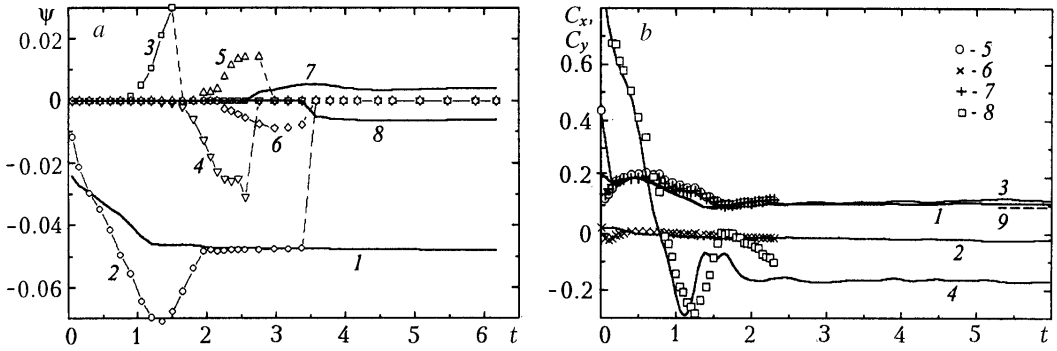

Fig. 6. Evolution of the mass flow rate under the profile (1) and the intensity of the vortices (2–8) in the wake of the automobile profile with time (a); comparative analysis of the time dependence of the drag coefficient of the profile and its components supplemented with the normal-force coefficient (b): 1, 5) C_x; 2, 6) C_{xp}; 3, 7) C_{xd}; 4, 8) C_y. Curves 1–4 are calculated with a time step of 0.03, and curves 5–8 are calculated with a step of 0.01. The experimental data 9 have been taken from [9, 10].

tex begins to dissipate immediately upon separating from the profile. However, it "lives" for a certain time and moves downstream. It should be noted that from the moment the starting vortex separates, the flow rate in the clearance between the profile and the screen ceases to increase linearly, in practice, and from this point on it remains constant.

The cyclic process of vortex formation in the case of flow around the profile (Fig. 4) is related to the alternate descending of vortices from both the upper convex part (similarly to a starting vortex) and the cut bottom part. In this case, the intensity of the vortices descending from the upper side exceeds the intensity of the oppositely swirled vortices. It is significant that each of the subsequent descending vortices is less intense than the previous ones and thus the von Kármán vortex street behind the automobile profile near the mobile screen turns out to be degenerate. Finally, two attached large-scale vortices are left in the near wake of the profile. Although a fairly long process covering the period from 1.2 to 6.17 is considered in Fig. 4, approximately from $t = 3.3$ the evolution of the vortex structure occurs only due to a small deformation of the separation zone behind the profile and due to the damping of the vortex flow in the far wake.

The combined analysis of the evolution of the distributions of C_p and C_f over the contour of the profile presented in Fig. 5 shows that, on the one hand, from approximately $t = 2.5$ the considered distributions of the local force characteristics are frozen even though the nonstationary processes of vortex formation and vortex transfer continue. On the other hand, the process which is related to the propagation of pressure and friction waves develops (we called your attention to it earlier). It is of interest that the pressure waves are enhanced on passage to the extending part of the clearance. Their amplitude is very large for a certain time (of the order of 0.5). After $t = 2.15$, the waves degenerate.

The time dependences of the integral force characteristics for the automobile profile are presented in Fig. 6b. Quite a satisfactory agreement between the calculation results at $\Delta t = 0.03$ and 0.01 points to the acceptability of the selected time step. The transient process is best illustrated by the behavior of the normal-force coefficient C_y that changes within fairly large limits and whose value becomes stabilized approximately by $t = 3$. The last-mentioned estimate corresponds well to the above moment of damping of the vortex pattern of flow around the automobile profile.

As is noted in [3], when stationary flow around a profile is considered, its drag is determined practically completely by the contribution of the base drag. The other components have a much smaller (by an order of magnitude) specific weight. It should be noted that the calculated drag coefficient is very close to the experimental one taken from [9, 10]. At the same time, the pattern of nonstationary flow around the profile, which is close to the asymptotic pattern, differs only slightly from the analogous pattern of stationary flow around the profile [3].

The work was carried out with financial support from the Russian Foundation for Basic Research (project Nos. 02-01-00670, 02-02-81035, and 02-01-01160).

NOTATION

t, time; Δt, time step; s, distance measured clockwise along the contour of the profile in fractions of the chord; C_p, pressure coefficient; C_f, coefficient of friction; Re, Reynolds number; ψ, stream function; C_x, C_{xp}, C_{xd}, and C_y, drag coefficient, profile-drag coefficient, base-drag coefficient, and normal-force coefficient.

REFERENCES

1. S. A. Isaev, N. A. Kudryavtsev, and A. G. Sudakov, *Inzh.-Fiz. Zh.*, **71**, No. 4, 618–631 (1998).
2. S. Ya. Grabarnik and S. A. Isaev, *Inzh.-Fiz. Zh.*, **71**, No. 5, 872–879 (1998).
3. S. A. Isaev, *Inzh.-Fiz. Zh.*, **73**, No. 3, 600–605 (2000).
4. I. A. Belov and N. A. Kudryavtsev, *Heat Transfer and Resistance of Tube Banks* [in Russian], Leningrad (1987).
5. I. A. Belov, S. A. Isaev, and V. A. Korobkov, *Problems and Methods of Calculation of Separated Incompressible Fluid Flows* [in Russian], Leningrad (1987).
6. V. L. Zhdanov, S. A. Isaev, and H.-J. Niemann, *Inzh.-Fiz. Zh.*, **74**, No. 5, 36–38 (2001).
7. S. A. Isaev, V. L. Zhdanov, P. A. Baranov, and V. B. Kharchenko, *Numerical Modeling of Laminar and Turbulent Flows Past a Circular Cylinder with Inner Channels and Windows in the Circuit* [in Russian], Preprint No. 3 of the A. V. Luikov Heat and Mass Transfer Institute of the National Academy of Sciences of Belarus, Minsk (2002).
8. I. A. Belov and S. A. Isaev, *Modeling of Turbulent Flows*: *Textbook* [in Russian], St. Petersburg (2001).
9. R. Buchheim, H. Rohe, and H. Wusteberg, *Volkswagen. Forschung-neue Technologien. Sonderdruck aus ATZ Automobiltechnische Zeitschrift*, **91**, No. 11 (1989).
10. K. Kitoh, T. Kobayashi, and H. Morooka, in: *Proc. Int. Conf. "Computational Mechanics-86: Theory and Applications,"* Tokyo (1986), pp. 77–82.